Cretaceous Research 144 (2023) 105458

Contents lists available at ScienceDirect

Cretaceous Research

journal homepage: www.elsevier.com/locate/CretRes

Ornithopod diversity in the Lower Cretaceous of Spain: New styracosternan remains from the Barremian of the Maestrazgo Basin (Teruel province, Spain)

E. Medrano-Aguado [a, *], J. Parrilla-Bel [a], J.M. Gasca [b], A. Alonso [a], J.I. Canudo [a]

[a] Grupo Aragosaurus – IUCA, Facultad de Ciencias, Universidad de Zaragoza, C/ Pedro Cerbuna, 12, 50009 Zaragoza, Spain
[b] Departamento de Geología, Universidad de Salamanca, Plaza de los Caídos, s/n, 37008 Salamanca, Spain

ARTICLE INFO

Article history:
Received 23 September 2022
Received in revised form
15 December 2022
Accepted in revised form 18 December 2022
Available online 26 December 2022

Keywords:
Dinosauria
Iguanodontia
Blesa Formation
Ilium
Iberian Peninsula

ABSTRACT

New material of an iguanodontid styracosternan ornithopod from the Lower Cretaceous of the Iberian Peninsula is described. The cranial and postcranial skeletal remains are from the Barranco del Hocino-1 site. These fossils (Iguanodontidae *sensu* Xu et al., 2018) represent the first medium-sized styracosternan from the Upper Sequence of the Blesa Formation (Barremian). The new material is characterized by a unique combination of characters that suggest they correspond to a new taxon: the first caudal vertebra with a ventral keel, the ilium with the preacetabular process twisted along its long axis, the dorsal surface of the preacetabular process and the main body totally straight and slender, the dorsal surface above the ischiadic peduncle slightly swollen but not forming a bulge or everted rim over the main body, and the ventral surface of the ischiadic peduncle and the postacetabular process straight and parallel to the dorsal surface of the main body. The new material is part of a vertebrate fossil assemblage of disarticulated bones but it represents the most anatomically informative remains of an styracosternan of the Oliete subbasin and would be potentially a distinct taxon. Regarding the new material along with the seven known taxa, the fossil record from the Barremian of the Iberian Peninsula depicts the existence of great diversity and abundance of ornithopod dinosaurs during the Early Cretaceous in the southwest of Europe, indeed greater than in other regions and thus aiming to be a relevant paleogeographic scenario for the evolutionary history of the group.

© 2022 The Authors. Published by Elsevier Ltd. This is an open access article under the CC BY-NC-ND license (http://creativecommons.org/licenses/by-nc-nd/4.0/).

1. Introduction

Iguanodontia is a clade of ornithopod dinosaurs that diversified markedly during the Early Cretaceous, especially in Laurasia (Weishampel et al., 2004; Carpenter and Ishida, 2010; Godefroit et al., 2012; McDonald, 2012; Norman, 2013; Boyd, 2015). Within Iguanodontia, styracosternans (*sensu* Sereno, 1986) are especially abundant and diverse in the Lower Cretaceous record of Europe, with fossil occurrences in Spain, England, Belgium, Portugal and other countries (e.g., Godefroit et al., 2009; Norman, 2013; Lockwood et al., 2021; García-Cobeña et al., 2022; Gasulla et al., 2022; Rotatori et al., 2022). The general anatomy of the group is especially conservative (Weishampel et al., 2004), which contributed to its diversity being underestimated for many years. The remains of styracosternans were thus traditionally assigned to the best-known species (i.e., *Iguanodon bernissartensis* and *Mantellisaurus atherfieldensis*: see Paul, 2008; Lockwood et al., 2021), despite there being some discrepancy concerning anatomical features, the palaeogeographical context and age.

The significant diversity of ornithopods during the Early Cretaceous of the Iberian Peninsula was noted by Canudo et al. (2010) in La Cantalera-1 site (Teruel), where four different ornithopod taxa have been identified from isolated teeth. Subsequently, Gasca et al. (2014) differentiated three iguanodontian maxillary tooth morphologies at this fossil site. This indicates notable diversification among these dinosaurs from the Iberian Peninsula compared to the rest of Europe. *Iguanodon bernissartensis* has been identified in the Morella (Gasulla et al., 2022) and Tragacete formations (Sanguino and Buscalioni, 2018), whereas specimens closely related to *Mantellisaurus atherfieldensis* have been reported in the Morella (Gasulla, 2015) and La Huérguina (Serrano et al., 2013) formations. In addition, several styracosternan taxa from the upper

* Corresponding author.
E-mail address: emedranoaguado@unizar.es (E. Medrano-Aguado).

https://doi.org/10.1016/j.cretres.2022.105458
0195-6671/© 2022 The Authors. Published by Elsevier Ltd. This is an open access article under the CC BY-NC-ND license (http://creativecommons.org/licenses/by-nc-nd/4.0/).

Hauterivian-Albian record of Iberia have been described in recent years, such as *Iguanodon galvensis* in the Camarillas (Verdú et al., 2018) and El Castellar (García-Cobeña et al., 2022) formations, *Morelladon beltrani* in the Morella Formation (Gasulla et al., 2015), *Magnamanus soriaensis* in the Golmayo Formation (Fuentes Vidarte et al., 2016), *Delapparentia turolensis* in the Camarillas (Ruiz-Omeñaca, 2011) and Blesa (Gasca et al., 2015) Formations, *Portellsaurus sosbaynati* in the Mirambel Formation (Santos-Cubedo et al., 2021), and a tall-spined Iguanodontia indet. (Pereda-Suberbiola et al., 2011) may be related to Morelladon in the Pinilla de los Moros Formation.

From 2015 to 2019 five excavation campaigns were carried out in the Barranco del Hocino-1 site. On the basis of isolated teeth, at least two different styracosternans were identified at the site (Medrano-Aguado et al., 2021). Several disarticulated bones from a medium-large-sized ornithopod and some isolated theropod teeth were recovered, as well as a few ankylosaur dermal plate fragments (Alonso et al., 2016, 2018). Many crocodylomorph teeth are under revision at this moment (Parrilla-Bel et al., 2022). All these remains evidence the typical association of an animal carcass exploited by predators and scavengers.

The main objective of this paper is to describe the remains of an iguanodontian ornithopod recovered in the Barranco del Hocino-1 site (Teruel, Spain).

1.1. Geographical and geological context

The Barranco del Hocino-1 site is located in the municipality of Estercuel, 95 km northeast of the city of Teruel, Aragón, in eastern Spain. Geologically, the site is located in the basalmost part of the Upper Blesa Sequence of the Blesa Formation (Aurell et al., 2018) (Fig. 1). The Blesa Formation includes an up-to-150 m-thick siliciclastic-carbonate succession (Fig. 1C), which represents the earliest synrift sedimentary fill of the Oliete subbasin, in the northwestern part of the Maestrazgo Basin (Soria et al., 1995; Salas et al., 2001). Many vertebrate sites have been discovered since the 90 s decade. Some of them have been excavated and studied in recent years (Canudo et al., 2010; Alonso and Canudo, 2015; Parrilla-Bel and Canudo, 2015; Holgado et al., 2019). Recently, the Blesa Formation has been subdivided into three depositional sequences: the Lower, Middle and Upper Blesa sequences with continental (distal alluvial to lacustrine), transitional (shallow marine to coastal) and continental (distal alluvial to lacustrine) depositional environments respectively (Aurell et al., 2018). The discontinuity between the Middle-Upper sequences was the result of a regressive event that occurred under climatic control (Aurell et al., 2018), which determined the continental sedimentation of the Upper Sequence. Conglomerate and sandstone levels were described under the lutitic/marl levels of the Barranco del Hocino-1 site (Fig. 1C), proving the position of the bonebed in the Upper Blesa Sequence (Aurell et al., 2018).

The charophyte record, including the presence of *Atopochara trivolvis triquetra* identified in different outcrops of the Lower Blesa Sequence, is indicative of the early to mid-late Barremian (Riveline et al., 1996; Aurell et al., 2018). In the Barranco del Hocino-1 site a Barremian charophyte assemblage formed by the clavatoraceans *Atopochara trivolvis triquetra*, *Globator maillardii trochiliscoides* and *Globator maillardii biutricularis* has been recovered (Alonso et al., 2016). The overlying Alacón Formation (Fig. 1B) has recently been reevaluated, and the Barremian-Aptian boundary is apparently lost due to a sedimentation gap between the Alacón and Forcall formations (García-Penas et al., 2022). Taking into account the aforementioned data, we consider the Barranco del Hocino-1 site to be chronostratigraphically placed near the boundary between the early and late Barremian.

The Barranco del Hocino-1 site is located within an alternation of limestones and lutitic/marly levels, where two different fossiliferous horizons have been identified (Alonso et al., 2018). The main vertebrate-bearing interval is 1 m thick and consists of grey lutites with different-coloured mottling (red, green, yellow, purple), bioturbation and carbonate nodules (Alonso et al., 2016, 2018). Aurell et al. (2018) interpreted the depositional environment as a palustrine area within a distal alluvial plain and with palaeosol development. Most of the recovered fossils show evidence of transport and weathering, and sometimes bioerosion (i.e. invertebrate or tooth traces) (Alonso et al., 2016). Vertebrate remains of different groups are common in this site: osteichthyan scales, crocodylomorph teeth and osteoderms, bones of testudines, dinosaur (ornithopod, theropod and ankylosaur) bones, as well as abundant coprolites and scarcer eggshell fragments (Alonso et al., 2016; Aurell et al., 2018).

2. Material and methods

The fossil material from the Barranco del Hocino-1 site was recovered during fieldwork campaigns from 2015 to 2019 carried out by the Aragosaurus-IUCA research team (University of Zaragoza). The fossil restoration was carried out by the authors in the palaeontological laboratory of the University of Zaragoza with mechanical methods. The studied material is housed in the Museo de Ciencias Naturales de la Universidad de Zaragoza (MPZ), Spain (Canudo, 2018). For the phylogenetic analysis, we used the modified version of Rotatori et al. (2022) based on the Xu et al. (2018) matrix. The data matrix was compiled in Mesquite v. 3.61 (Maddison and Maddison, 2018) and analysed in TNT v.1.5 (Goloboff and Catalano, 2016).

3. Comment on taphonomy

Several fossils from different vertebrates come from the Barranco del Hocino-1 site. The bedform could be subdivided into three different sedimentological levels: top level with large but very fragmented bones, medium level with coprolites and some crocodylomorph teeth and bottom level, the most fossiliferous one. The new material herein described comes from this level. The fossil remains recovered have different preservation states. Bone fragments and incomplete but identifiable bones are common in this level, but also complete and well preserved dinosaur bones have been recovered, some of them very close to each other (e.g. some dorsal ribs and one left ilium of an ornithopod dinosaur). The bones are disarticulated and many of them have weathering and before burial fractures, evidence of subaerial exposure.

Some bones have tooth marks that could be related with crocodylomorph and dinosaur scavenger behaviour. Aquatic invertebrate galleries are present in the surface of some bones or over the sediment attached to the bone evidence of subaquatic exposition. For this work we selected the complete ornithopod fossils that have been recovered from the bottom sedimentological level and with a good preservation condition. The preservation is consistent across the selected fossils and controversial bones like fragments of ribs, vertebrae or long bones have been discarded for this paper due to the lack of taxonomy information they provide. A more detailed taphonomy paper is planned to understand the different processes that have taken place over the time and form Barranco del Hocino-1 site.

4. Systematic palaeontology

Dinosauria Owen, 1842
Ornithischia Seeley, 1887

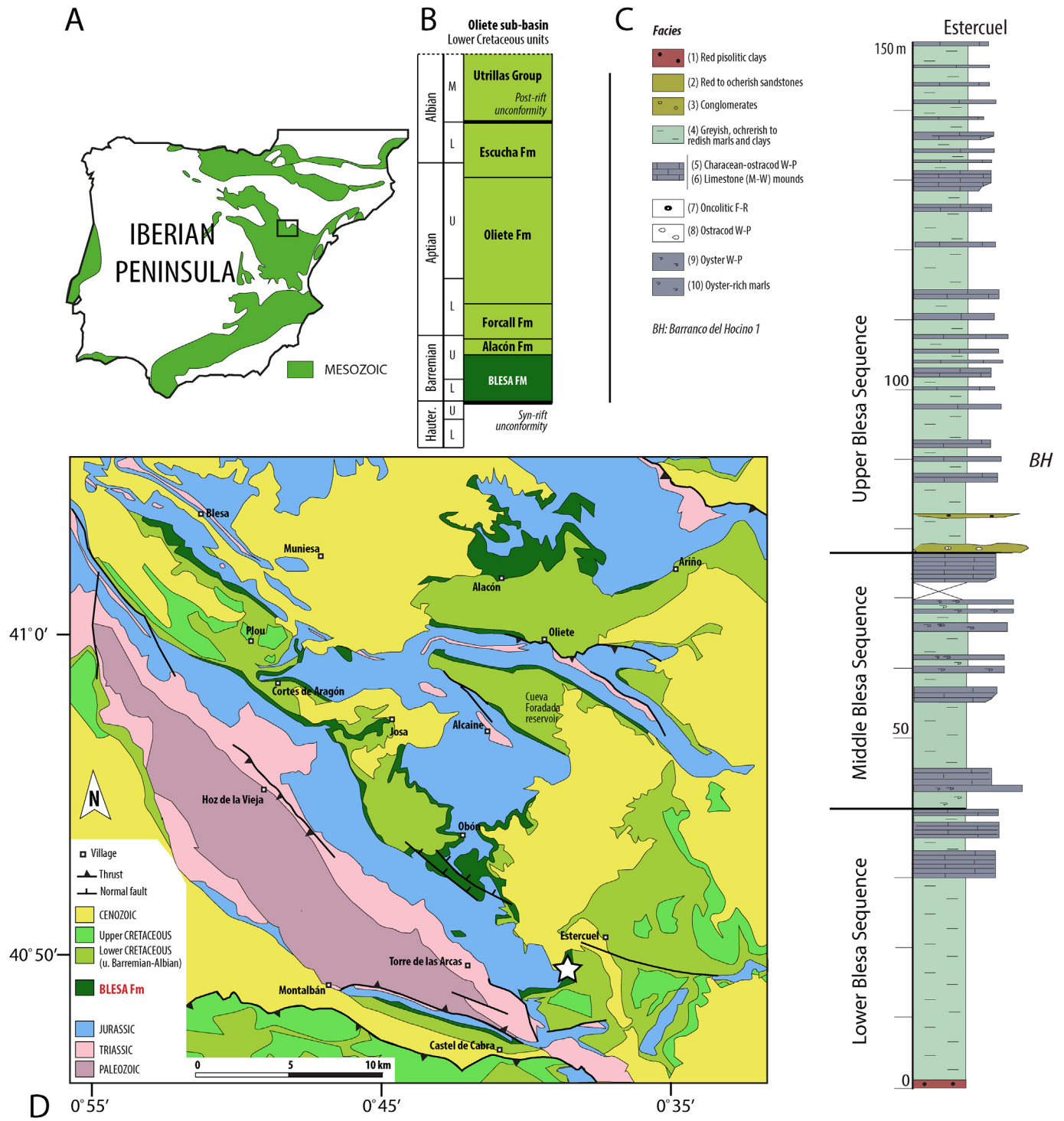

Fig. 1. Geographical and geological situation of the Barranco del Hocino-1 site (Teruel, Spain). A: Iberian Peninsula with Mesozoic basins in green. The square indicates the location of the Oliete subbasin. B: Lower Cretaceous formations of the Oliete subbasin (modified from Aurell et al., 2018). C: stratigraphic section of the Blesa Formation in Estercuel (modified from Aurell et al., 2018). See the Barranco del Hocino-1 site above the conglomerate level that indicates the base of the Upper Blesa Sequence. D: Geological map of the Oliete subbasin with the Blesa Formation as well as the rest of the Lower Cretaceous formations (modified from Aurell et al., 2018). Star indicates the Barranco del Hocino-1 site. (For interpretation of the references to colour in this figure legend, the reader is referred to the Web version of this article.)

Ornithopoda Marsh, 1881
Iguanodontia Sereno, 1986
Ankylopollexia Sereno, 1986
Styracosterna Sereno, 1986

Locality and horizon. Upper Blesa Sequence, Blesa Formation; Barremian, Lower Cretaceous (Aurell et al., 2018). Estercuel, Teruel, Aragón, Spain.

Material. Some vertebra fragments, three caudal vertebrae (MPZ 2022/728, 2022/729 and 2022/730), four complete dorsal ribs (MPZ

2022/731, 2022/732, 2022/733 and 2022/734) and several rib fragments, some sacrum fragments, left ilium (MPZ 2022/735), partial left tibia (MPZ 2022/736). Figs. 2-5.

5. Description

5.1. Vertebrae

MPZ 2022/729 is the first caudal vertebra (Fig. 2A-D). The centrum is platycoelous and preserves its original shape, but anterior and posterior surfaces are partially eroded. The neural arch and transverse processes are practically lost. The centrum is 95 mm high, 90 mm wide and 65 mm long. The anterior articulation face is subrounded, wider in the dorsal half than in the ventral half (Fig. 2A). Only the beginning of the neural arch is preserved. The lateral surfaces present some small foramina. Invertebrate galleries are attached to the sediment of the neural canal (see section 3: Comment on taphonomy). There is a long and slender tooth mark in the right lateral surface of the centrum (Fig. 2B). The anterior surface is flat in the ventral half and slightly convex in the dorsal half. This morphology (described in the first caudal vertebra of *Iguanodon bernissartensis* (Norman, 1980) and *Brighstoneus simmondsi* (Lockwood et al., 2021)) and the absence of articulation facets for the chevrons indicate that it is the first caudal vertebra. The posterior articulation face (Fig. 2C) is more rounded than the anterior one and slightly concave. The lateral surface is smooth, concave anteroposteriorly and convex dorsoventrally between the articulation surface edges. These edges are rounded and slightly everted. The ventral surface of the centrum is eroded but has a single ventral keel (Fig. 2D).

MPZ 2022/728 is a platycoelous anterior caudal vertebra centrum (Fig. 2E-H). The centrum is nearly complete, but the ventral and anteroventral surfaces are partially eroded and the posterior face is almost completely eroded. The neural arch and transverse processes are not preserved. The centrum is higher (90 mm) than it is wide (75 mm) and long (75 mm). The anterior articulation face (Fig. 2E) is quadrangular in shape and slightly concave. In lateral view (Fig. 2F) the centrum has a rectangular morphology, and its surface is smooth, slightly concave anteroposteriorly and convex dorsoventrally. The edges of the articulation faces are slightly everted and rounded, but they are quite eroded. The posterior articulation face is of an inverted triangular shape (Fig. 2G) but this could be due to taphonomic processes. On the anteroventral surface of the centrum are the articulation facets for the chevron, which are poorly preserved. The ventral surface is slender and probably had a keel structure, but this surface is eroded (Fig. 2H). Only the insertion of the neural arch with the centrum is preserved, and the ventral section of the neural canal can be recognised. Both lateral surfaces have a small foramen near the ventral edge.

MPZ 2022/730 is a caudal vertebral centrum. The articular surfaces are almost wholly eroded; only parts of the lateral surfaces and the ventral surface of the neural canal are preserved. The neural arch is completely lost. The centrum is 70 mm high, 60 mm wide and 82 mm long. The centrum is rectangular in shape in anterior and posterior view. The ventral surface is thinner than the rest, but due to the poor state of preservation it is impossible to recognise the presence or absence of a ventral keel or the attachment facets for the chevron. The neural canal is subrounded.

5.2. Ribs

More than 30 rib fragments have been recovered. Most of them are fragments of the shaft of dorsal ribs. MPZ 2022/731 and MPZ 2022/732 are two dorsal ribs that are nearly complete (Fig. 3). MPZ 2022/731 shows a possible tooth mark in the capitulum, whereas MPZ 2022/732 has some tooth marks in the distal end. They are

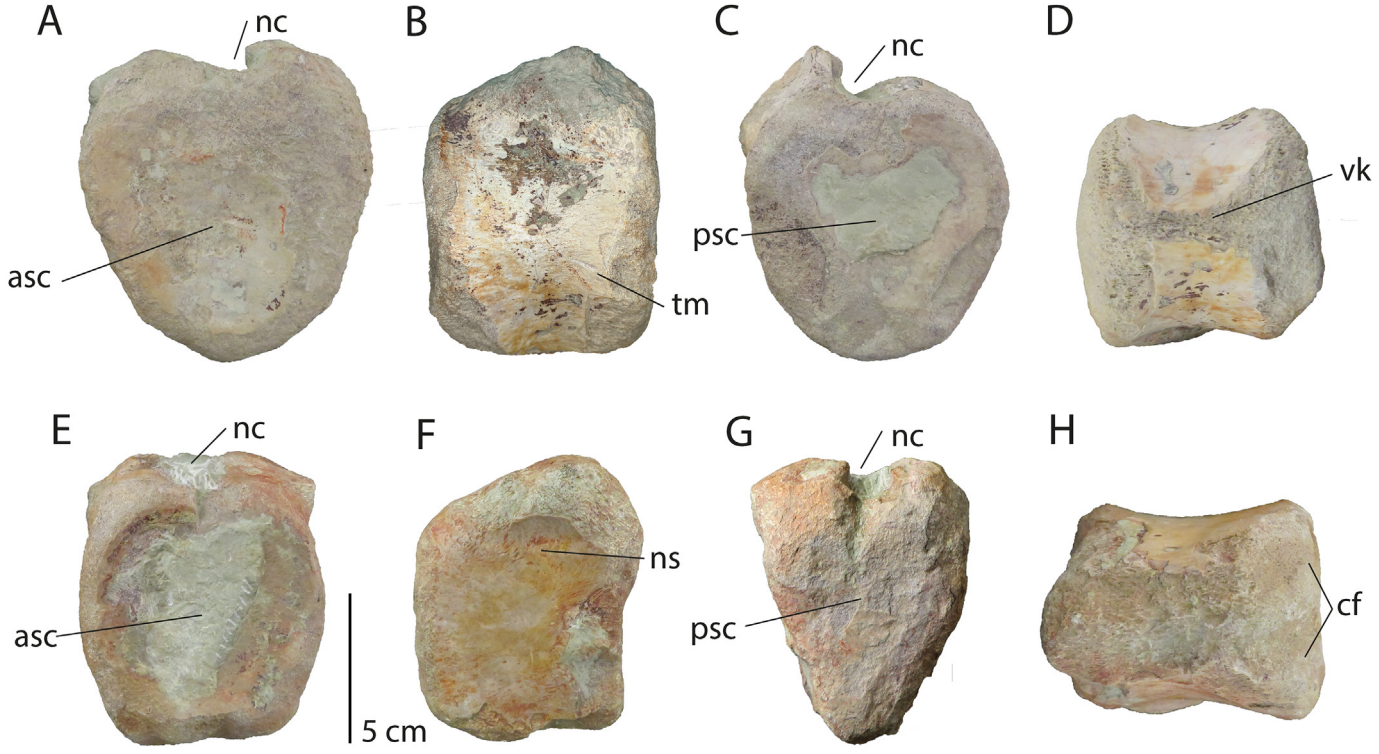

Fig. 2. Caudal vertebrae. MPZ 2022/729 in A: anterior view. B: right lateral view. C: posterior view. D: ventral view. MPZ 2022/72 in E: anterior view. F: left lateral view. G: posterior view. H: ventral view Abbreviations: asc, anterior surface of the centrum; cf, chevron facet; nc, neural canal; ns: neural suture; psc: posterior surface of the centrum; tm: tooth mark; vk: ventral keel.

anterior right dorsal ribs, but it is not possible to place the ribs accurately in their specific position. These ribs are probably the longest of the rib series, it being nearly 80 cm from the capitulum to the end of the shaft, which is not totally preserved. The capitulum is flattened anteroposteriorly and has an oval morphology, with the long axis dorsoventral. The dorsal surface of the capitulum points slightly forward and is almost flat. The capitulum is wider than the neck of the rib. The tuberculum rises above the neck by 10 mm and has an articulation facet that is concave medially and slightly posteriorly directed. The neck is anteroposteriorly slender with the ventral surface curved, and the dorsal surface is full of scars for the ligaments of the transverse process of the vertebra (Fig. 3I, J). The surface with the scars is totally dorsally oriented and has a slight ridge that crosses from the anterodorsal part of the capitulum to the posteromedial part of the tuberculum. The longitudinal ridge of the anterior surface (Fig. 3B, D) is well developed from the tuberculum to the midpoint of the medial edge of the shaft, giving it a triangular morphology in cross section. At the end of the ridge the shaft narrows mediodistally, and at the distal end it flattens and thickens slightly, showing a blunt spatulate end, which could be the articulation with the sternal cartilaginous ribs (Norman, 1980). In the posterior surface there is a small ridge near the lateral edge under the tuberculum, creating a little flange (Fig. 3A, C). The union point between the tuberculum and the shaft shows a concave morphology. Both anterior dorsal ribs formed a 90-degree angle between the capitulum and the shaft.

MPZ 2022/733 is a left posterior rib with less curvature than the anterior ribs. The morphology of the capitulum is similar to those described above (MPZ 2022/731 and MPZ 2022/732). The neck is anteroposteriorly thicker than the anterior ones (Fig. 3K) and the ligament attachment scars are delimited to a flat surface located dorsoposteriorly. This surface is relatively bigger than the anterodorsal rib surface and strongly marked. It is located slightly ventrally, making the tuberculum bigger and raising it above the neck. The shaft is rounded, and the anterior ridge is gentle, whereas the posterior ridge is marked.

MPZ 2022/734 is a right posterior dorsal rib too. It is slimmer, more rounded, and shorter than the other complete ribs. There is a rounded collapse morphology near a fracture at the beginning of the shaft, which was probably formed before the fracture. The capitulum is not widened (Fig. 3L), and the tuberculum rises less than in MPZ 2022/733, but the articulation facet is more backward-pointing. All the dorsal and posterodorsal surface are full of attachment scars, and there are gentle scars in the anterior surface too. The anterior surface ridge is smooth and rounded, whereas the posterior one forms a flange of 9 cm along the lateral edge. The shaft goes from rounded to a 'figure-of-eight-shaped' cross-section in the area of the ridge to flat at the distal end. There is a small foramen under the tuberculum in the posterior surface.

5.3. Ilium

MPZ 2022/735 is a left ilium that is nearly complete and generally well preserved (Fig. 4) with the exception of a broken and deformed postacetabular process that make it impossible to describe the characters in this part. Tooth marks can be recognised in the ventral part of the medial ridge and three more in the fragmented part of the lateral face near the ischiadic peduncle. There are at least two invertebrate feeding traces above the base of the medial ridge.

Its total preserved length anteroposteriorly is 684 mm from the end of the preacetabular process to the end of the postacetabular process and dorsoventrally 191 mm high measured at the ischiadic peduncle. The preacetabular process is long, straight and anteriorly directed. It curves slightly laterally. The anterior edge is apparently broken, and the total length is uncertain (230 mm preserved). The preacetabular process is dorsoventrally compressed and twists around its long axis with the lateral surface to face more dorsolaterally (Fig. 4A), which is a character seen in many iguanodontians (Norman, 2015). The posterior ventral face of the preacetabular process is triangular in cross-section due to the ridge for the articulation facet of the first sacral rib. This medial ridge is oriented medioventrally and is triangular in cross-section at the base of the preacetabular process, which slightly turns into a sheet toward the anterior edge. In lateral view the preacetabular process is almoststraight, like the main body of the ilium. The medial ridge from the articulation facet of the first sacral rib is visible in lateral view (Fig. 4B).

The main body of the ilium is relatively square (with the same dimension dorsoventrally as anteroposteriorly). In dorsal view, the preacetabular process curves laterally, while the postacetabular process curves medially (Fig. 4C, D). The dorsal edge of the main body is dorsoventrally straight and narrow. It is transversely rounded, thin and full of muscle scars above the pubic and ischiadic peduncle (Fig. 4A), and a portion is broken above the ischiadic peduncle. The pubic peduncle is large and flattened with a pubic articulation facet directed anteriorly and slightly dorsally. This surface is straight, rough and circular. The ischiadic peduncle has a rough and straight ventral surface that is wider than the rest of the ventral margin. In the medial surface, above the peduncle and directed posteriorly there is a muscle attachment surface with a semicircular morphology. The articular surface of the acetabulum starts at the anterior end of the pubic peduncle and continues posteriorly as a ridge that disappears above the ischiadic peduncle, describing a semicircular morphology (Fig. 4B). The ischiadic peduncle articulation surface is subcircular and ventrally directed. It does not form a stepped boss, and the ventral surface is parallel to the dorsal margin and the postacetabular ventral margin. The lateral surface of the main body is slightly convex, and the medial surface is slightly concave. The total length of the postacetabular process is 280 mm. The dorsal edge of this process curves downward, and the ventral edge is straight behind the ischiadic peduncle. The postacetabular process is crushed lateromedially, and no brevis shelf, fossa or ridge can be identified. The ventral surface of this process is less distorted than the rest of the process and is curved medially toward the main body of the ilium (Fig. 4D). The dorsal region of the lateral surface of the main body is slightly swollen and gently curved laterally above the ischiadic peduncle and posteriorly.

Four attachment points for the transverse processes and the dorsal part of the sacral ribs are recognised on the medial surface (Fig. 4A). The first attachment point is located on the ventral surface of the medial ridge of the preacetabular process. The second attachment point appears on the main body, adjacent to the base of the medial ridge. In continuity with the second, the third attachment point can be recognised. It has an oval morphology, with the long axis oriented anteroposteriorly, surrounded by small ridges. The last of the attachment points is above and posterior to the ischiadic peduncle. This one has a circular morphology, is bigger, and its surrounding ridge is more accentuated. These attachment points form a large ridge from the medial ridge of the preacetabular process to the end of the last attachment point described. Posterior and ventral to these facets the surface of the ilium is heavily scarred in the area which serve as attachment for the sacral yoke. This ridge forms small peaks between each attachment point. Ventral to this ridge, in the anterior half of the main body of the ilium, concave subcircular depressions can be recognised, probably for the connection with the sacral yoke.

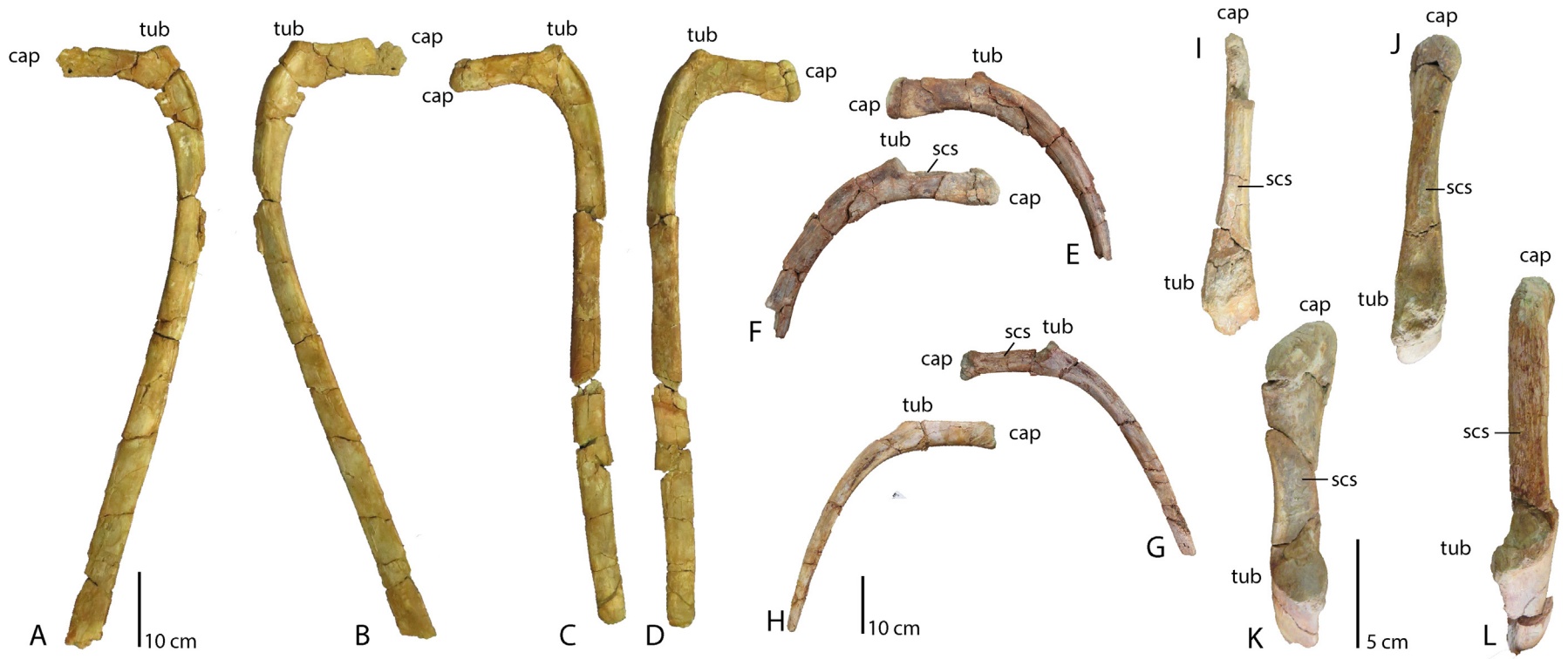

Fig. 3. Dorsal Ribs. MPZ 2022/731 in A: posterior view. B: anterior view. I: dorsal view. MPZ 2022/732 in C: posterior view. D: anterior view. J: dorsal view. MPZ 2022/733 in E: anterior view. F: posterior view. K: dorsal view. MPZ 2022/734 in G: posterior view. H: anterior view. L: dorsal view. Abbreviations: cap: capitulum; scs, scar surface; tub, tuberculum.

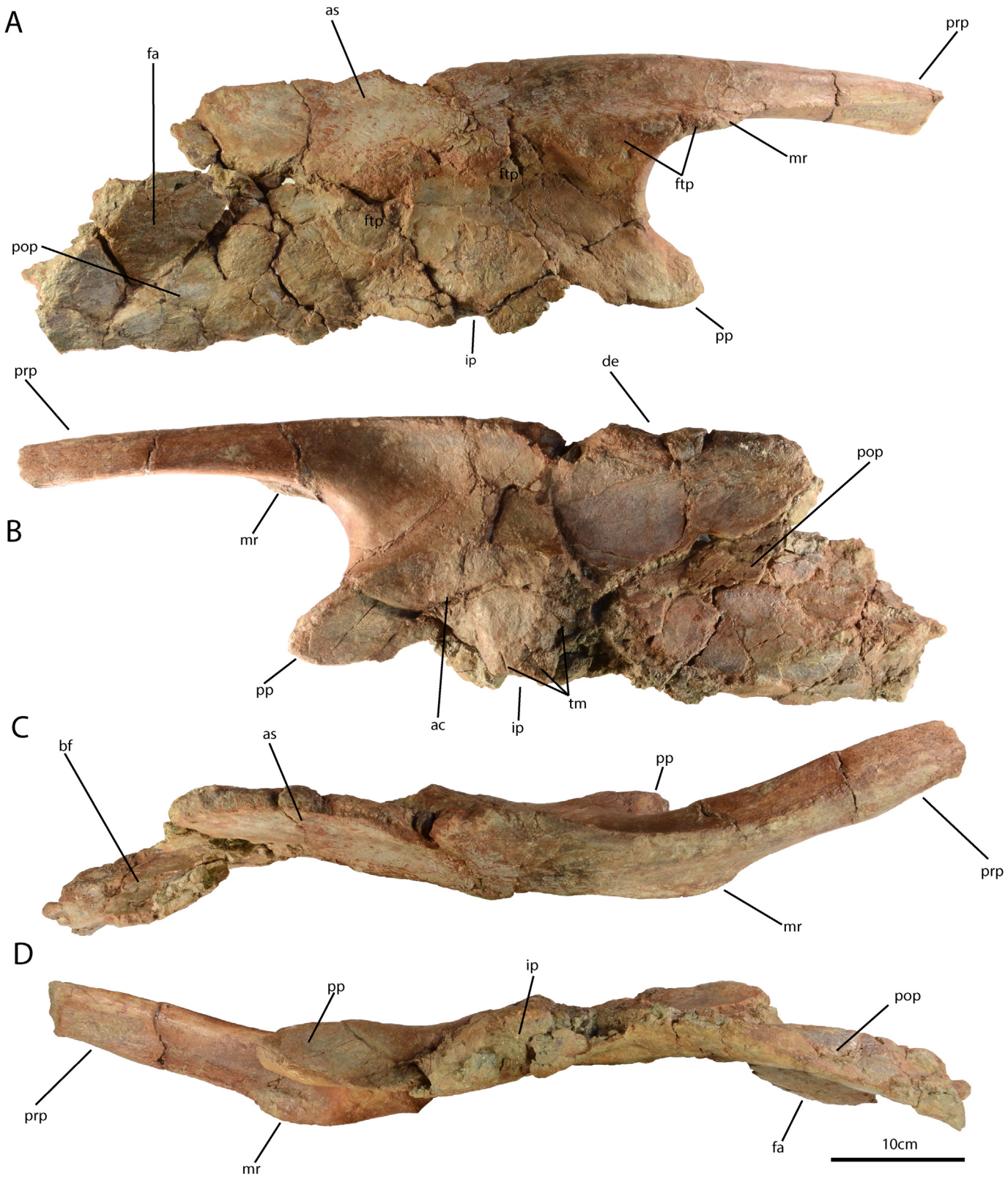

Fig. 4. Left ilium. MPZ 2022/735 in A: medial view. B: lateral view. C: dorsal view. D: ventral view. Abbreviations: ac, acetabulum; as, attachment scar surface; bf, brevis shelf; de, dorsal edge; fa, fragmented area; ftp, facet for transverse process; ip, ischiadic peduncle; mr, medial ridge; pop, postacetabular process; pp, pubic peduncle; prp, preacetabular process; tm, tooth marks.

5.4. Tibia

MPZ 2022/736 is a proximal fragment of the left tibia (Fig. 5). All the surfaces are eroded except the medial and posterior ones, and the cnemial crest is poorly preserved. Some invertebrate traces are visible in the sediment on the bone. The measurements of the fragment are a maximum length of 117 mm and a maximum width of 88 mm. The cnemial crest seems to be craniocaudally short and relatively wide mediolaterally, but the thin edge that surrounds the fibula is lost (Fig. 5A). The lateral and posteromedial condyles seem to be similar in size, and the cleft that separates them is deep and half as wide as the condyles.

6. Discussion

6.1. Ontogenetic stage

The neurocentral suture of the caudal vertebra is totally closed (Fig. 2F), and the sacral fragments show evidence of fusion between the vertebrae. Both features are considered evidence of changes that occur during the growth of ornithopods (Horner et al., 2004; Verdú, 2017; Hübner, 2018). In some senile specimens the fusion of the transverse process of the dorsal vertebrae and the neck of the dorsal ribs is typical (Verdú et al., 2018). There is no evidence of fusion between the ribs and the transverse process in any of the rib fragments recovered in the Barranco del Hocino-1 site. In light of these features we consider the material described before as belonging to a subadult or adult specimen.

The size of the bones recovered and the presumed subadult or adult ontogenetic stage of the specimen suggest that this taxon is a medium-sized styracosternan (estimated body length about 6 m based on ilium and vertebrae) like the coetaneous *Morelladon beltrani* or *Mantellisaurus atherfieldensis*, and smaller than *Iguanodon bernissartensis*.

6.2. Comparative anatomy

The large bones found in the Barranco del Hocino-1 site (from MPZ 2022/727 to 2022/736) are identified as belonging to a styracosternan iguanodontian due to the following characters. The anterior caudal vertebrae have a centrum that is platycoelous or near-amphiplatyan and is slightly anteroposteriorly compressed with a sinuous suture with the neural arch. These are characters typical of Ornithopoda (Norman, 2004; Pereda-Suberbiola et al., 2011). The long preacetabular process of the ilium is typical of iguanodontian ornithopods. The preacetabular process of the ilium twisted along its long axis is a synapomorphy of Iguanodontoidea (Verdú, 2017). A relatively straight, thickened and slightly everted dorsal margin of the main body of the ilium is characteristic of non-hadrosaurid iguanodontians, whereas more derived ornithopods show a pendant lip (Norman, 2004).

Here we compare the fossils of Barranco del Hocino-1 site with all coeval basal styracosternans from Western Europe: *Iguanodon bernissartensis*, *Iguanodon galvensis*, *Morelladon beltrani*, *Delapparentia turolensis* (considered *nomen dubium*, Norman, 2015; Verdú et al., 2018), *Proa valdearinnoensis*, *Magnamanus soriaensis*, *Barilium dawsoni*, *Hypselospinus fittoni*, *Brighstoneus simmondsi*, *Mantellisaurus atherfieldensis* and *Ouranosaurus nigeriensis*. There is no overlapping material to compare *Portellsaurus sosbaynati* with the described fossils.

General morphology of the caudal vertebrae is persistent in Iguanodontia (Weishampel et al., 2004). MPZ 2022/728, with a similar morphology and size to MPZ 2022/729, corresponds with the third or fourth caudal vertebra, to judge by the presence of chevron articulation facets in the anterior and posterior articulation surfaces. The presence of a single ventral keel in the first caudal is described in the styracosternan *Ouranosaurus nigeriensis* (Bertozzo et al., 2017), but not in the closely related styracosternans *I. bernissartensis*, *I. galvensis*, *B. dawsoni*, *M. soriaensis* or *B. simmondsi*. No caudal vertebrae have been described for *M. beltrani*.

The ribs are similar to those of *I. bernissartensis*, *I. galvensis*, *M. atherfieldensis*, *B. simmondsi*, *B. dawsoni*, *H. fittoni* and other related iguanodontians. The ratio between the dorsoventral length of the neck and the length from the capitulum to the tuberculum, as well as the morphology, size and swelling of the articular surfaces of the capitulum and tuberculum of MPZ 2022/731-734, are similar to *I. bernissartensis*, *I. galvensis*, *M. atherfieldensis*, *B. dawsoni* and *H. fittoni*, but are different from *B. simmondsi* and *M. beltrani*, especially the morphology of the tuberculum surface. This surface is wider, more rounded and more separated from the shaft of the rib in *M. beltrani* and *B. simmondsi* than in the other ornithopods cited previously. The ribs of *M. soriaensis* are poorly preserved and distorted.

The general morphology of the ilium is similar to that of *B. dawsoni*, *D. turolensis* and *I. galvensis* (Fig. 6). The dorsoventrally compressed preacetabular process is shared with *B. dawsoni*, *I. galvensis*, *I. bernissartensis* and *D. turolensis*, whereas this process is transversely compressed in other styracosternans such as *M. atherfieldensis*, *B. simmondsi*, *M. beltrani* and *O. nigeriensis*. However, the anterior end of the preacetabular process, although incomplete, is apparently tabulate and lacks evidence of swelling. This character differs from many of the basal hadrosauriforms, which have a boot-shaped end of the preacetabular process (i.e.,

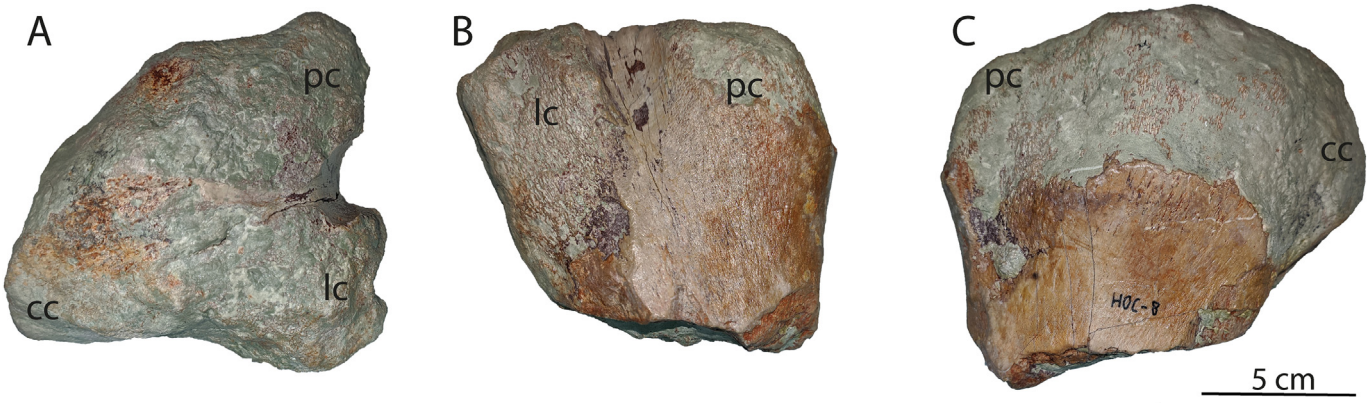

Fig. 5. Left tibia. MPZ 2022/736 in A: dorsal view. B: caudal view. C: medial view. Abbreviations: cc, cnemial crest; lc, lateral condyle; pc, posteromedial condyle.

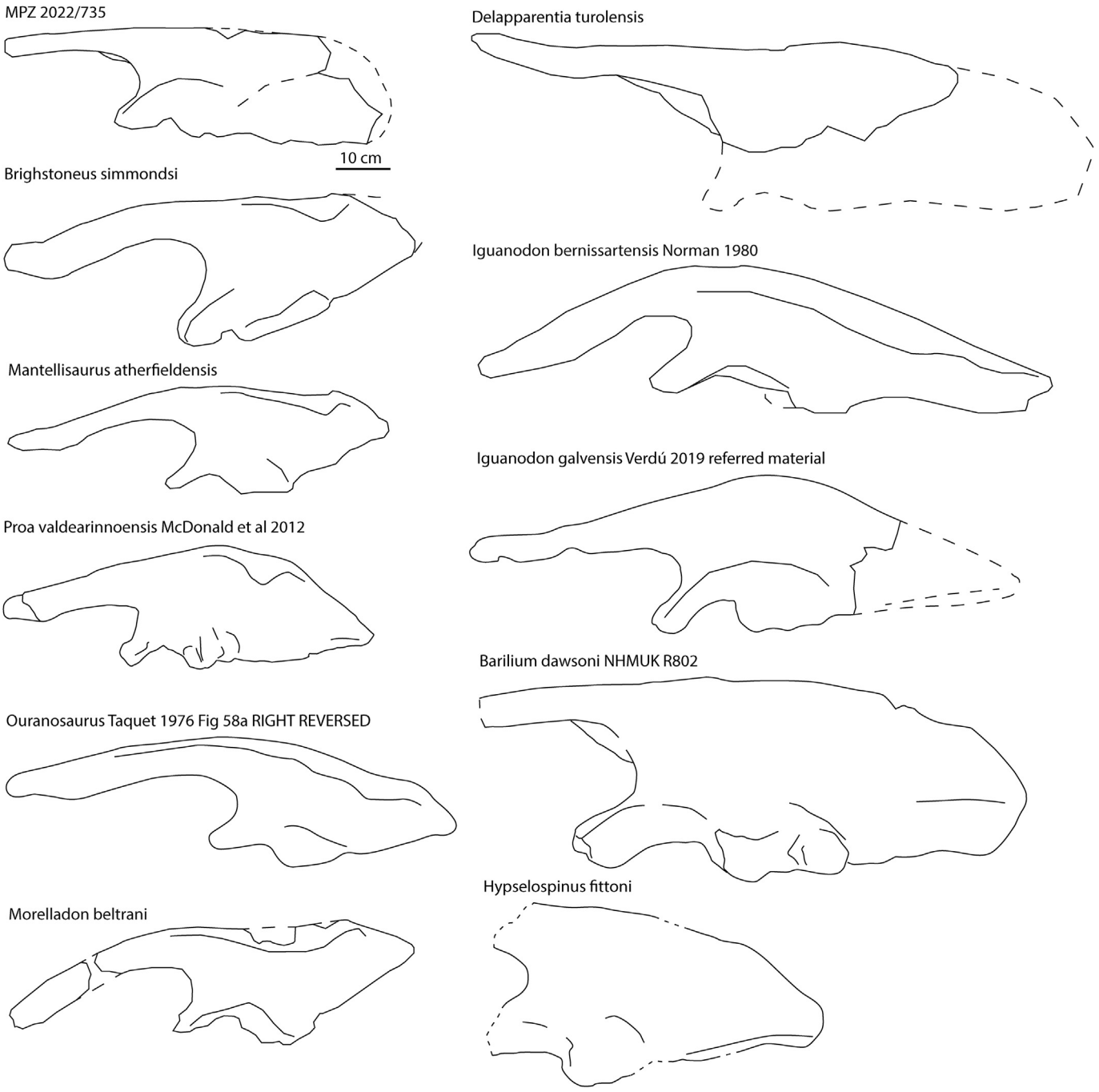

Fig. 6. Comparison of the ilia of medium and large size styracosternans from the Lower Cretaceous of Europe. Redrawing from: MPZ 2022/735, this paper; *Delapparentia turolensis*, holotype MPT/I.G. 473; *Brighstoneus simmondsi*, Fig. 19E in Lockwood et al. (2021); *Iguanodon bernissartensis*, Fig. 63 in Norman (1980); *Mantellisaurus atherfieldensis*, Fig. 2A, C in McDonald (2012); *Iguanodon galvensis*, Fig. 17E in Verdú et al. (2019); *Proa valdearinnoensis*, Fig. 8A in McDonald et al. (2012); *Barilium dawsoni*, Fig. 8A in Norman (2011); *Morelladon beltrani*, Fig 12A in Gasulla et al. (2015); *Hypselospinus fittoni*, holotype NHMUK R163.

I. bernissartensis, *B. dawsoni*, *D. turolensis* and others), and it is only shared with *Tenontosaurus tilletti* (Forster, 1990), *Camptosaurus dispar* (McDonald, 2011) and *B. johnsoni* (Godefroit et al., 1998). The general shape and size of the medial ridge of the ilium is similar to *I. bernissartensis* (Norman, 1980), *I. galvensis* (Verdú et al., 2017), *H. fittoni* (Norman, 2015), but less developed than in *B. dawsoni* (Norman, 2011) and different from *B. simmondsi*, where the cross-section of the proximal part of the preacetabular process has the outline of a dorsoventrally expanded capsule instead of being triangular, which is the general shape in the other iguanodontians (Lockwood et al., 2021). The axial twisting of the preacetabular process is shared with *B. dawsoni* (Norman, 2011), *M. atherfieldensis*, *I. bernissartensis*, *I. galvensis*, *B. johnsoni* and *O. nigeriensis*, but this is absent in *B. simmondsi*, *H. fittoni* and *C. dispar*.

The dorsal border of the main body and the preacetabular process are straight, characters shared with *D. turolensis* and *B. dawsoni* (Fig. 6). However, the curvature and orientation of the

dorsal border have been considered as being subject to intraspecific variation in *I. bernissartensis* (Norman, 2015; Verdú et al., 2018) and *Gilmoreosaurus mongoliensis* (McDonald, 2010). The main body of the ilium is relatively square, as in *B. dawsoni* and *M. atherfieldensis*. It is more rectangular, with the long axis oriented anteroposteriorly in *I. bernissartensis*, *G. mongoliensis* and *Dryosaurus altus* but dorsoventrally in *B. simmondsi*, the genus *Zalmoxes* and *Hypsilophodon foxii* it is dorsoventrally oriented (Weishampel et al., 2003). Some non-hadrosaurid hadrosauriforms, such as *M. atherfieldensis*, *H. fittoni*, *Altirhinus kurzanovi*, *G. mongoliensis*, and all hadrosaurids have a posterolateral boss, but this is absent in MPZ 2022/735 and also in *M. beltrani*, *Proa valdearinnoensis*, the genus *Iguanodon* and *O. nigeriensis*.

The ischiadic peduncle does not form a stepped boss laterally, a diagnostic feature of *I. galvensis* (Verdú et al., 2017). The ventral surface is parallel to the dorsal margin and the postacetabular ventral margin, a character shared with *Iguanodon*, *Hypsilophodon foxii*, *Zalmoxes*, *Rhabdodon* and *Camptosaurus* (McDonald, 2011). The ventral margin of the ischiadic peduncle is inclined posterodorsally in the most derived hadrosauriforms and hadrosaurids and in *O. nigeriensis*, *Eolambia caroljonesa*, *Bactrosaurus johnsoni* and the recently described *Brighstoneus simmondsi* (Lockwood et al., 2021). In lateral view, the dorsal surface is slightly expanded and gently curved laterally above the ischiadic peduncle and posteriorly, as in *B. dawsoni*, *H. fittoni* and *D. turolensis*. Other basal hadrosauriforms have a more pendant process or a completely everted rim (i.e., *Iguanodon*, *M. beltrani*, *M. atherfieldensis*, *O. nigeriensis* and more derived hadrosauriforms).

The acetabular component of the ilium forms a semicircular surface that goes from the pubic peduncle to above the ischiadic peduncle. A similar morphology is seen in *I. galvensis*, *M. atherfieldensis*, *B. simmondsi* and *B. dawsoni* (Norman, 1986, 2011; Verdú et al., 2018; Lockwood et al., 2021). A thin section of bone forms a straight ventral margin with scars between the peduncles, similar to the morphology seen in *B. dawsoni*, *I. galvensis* and *B. simmondsi* (Norman, 2011; Verdú et al., 2018; Lockwood et al., 2021), whereas in *I. bernissartensis*, *M. atherfieldensis* and *M. beltrani* this surface is concave in ventral view and without evidence of scars (Norman 1980, 1986; Gasulla et al., 2015). There could be a difference in the position of the femur attachment with the lip, being more lateral in MPZ 2022/735 and more ventral in *M. beltrani* and *M. atherfieldensis*.

As in *B. simmondsi*, and *M. atherfieldensis* four attachment facets for the transverse processes of the first four true sacral vertebrae could be recognised while only three facets are distinguishable in the ilium of *M. beltrani*. If we use these facets to count the number of sacral ribs we can assume that the sacrum could be formed by six true sacral vertebrae plus one dorsosacral as in *B. simmondsi*, *M. atherfieldensis*, *B. dawsoni*, *B. johnsoni* and *O. nigeriensis*. *M. beltrani* sacrum is formed by five sacral and one dorsosacral and the large sized *I. bernissartensis* and *I. galvensis* sacrum possess seven true sacral plus one dorsosacral. Only fragments of the sacrum have been recovered in the Barranco del Hocino-1 site. Better preserved and complete material is needed to confirm this assumption besides that the number of fused vertebrae in the sacrum could change during the ontogeny (Lockwood et al., 2021).

The ontogenetic state of the vertebrae and sacrum is related with an adult or subadult specimen and the size of the bones corresponds with medium size styracosternan like *M. atherfieldensis* or *M. beltrani* while the general morphology of the ribs and ilium are closely similar to the large sized styracosternan ornithopods *I. bernissartensis*, *I. galvensis* and *B. simmondsi*.

6.3. Phylogenetic analysis

To assess the evolutionary relationships of the fossils described within Iguanodontia we conducted a phylogenetic analysis using the modified version of Rotatori et al. (2022) based on the Xu et al. (2018) matrix. The analysis was run with 125 unordered, equally weighted characters and 43 taxa with the addition of Barranco del Hocino-1 site ilium (MPZ 2022/735). The analysis was carried out using TNT v.1.5 version (Goloboff and Catalano, 2016), performing a traditional search under the tree bisection reconnection (TBR) swapping algorithm, saving 100 trees per replication for 1000 replicates. The consistency index, rescaled consistency index and retention index were calculated using the TNT script STAT.RUN, and clade support using the TNT script BREMER.RUN and TNT bootstrap, set to 1000 replicates, reporting groupings found in >50% of pseudoreplicate datasets. The analysis results in 10 most parsimonious trees (MPTs) with a tree length of 340 steps. The consistency index is 0.579, the retention index 0.872, and the rescaled consistency index 0.505 (Fig. 7).

The addition of MPZ 2022/735 to the Rotatori et al. (2022) matrix does not change the topology of the strict consensus tree, MPZ 2022/735 being recovered at the base of Hadrosauriformes, in a large polytomy with Hadrosauroidea plus ten other taxa. In the ten MPTs, MPZ 2022/735 is always recovered either in a clade with *Barilium dawsoni*, *Iguanodon bernissartensis* and *Mantellisaurus atherfieldensis* – the monophyletic Iguanodontidae *sensu* Xu et al. (2018) – or in a nested succession, always more nested than *I. bernissartensis* and *B. dawsoni* but less than *M. atherfieldensis*.

To further increase the resolution of the consensus, we ran a second analysis using implied weights, with a concavity constant of 15 (Goloboff et al., 2008). MPZ 2022/735 is recovered as a member of Iguanodontidae *sensu* Xu et al. (2018), more nested than *Mantellisaurus atherfieldensis* and sister to the clade formed by *Iguanodon bernissartensis* and *Barilium dawsoni*.

This phylogenetic position is supported by the morphology of the dorsal edge of the ilium which is dorsoventrally thickened and laterally bulgy edges, forming a non-everted, weakly developed eminence. This character (102, 3 > 2) is shared with *B. dawsoni* and *I. bernissartensis* but not with *M. atherfieldensis*. However, it lacks the convex lateral profile of the dorsal edge of the main body of the ilium (character 101, 0 > 1).

6.4. Lower Cretaceous styracosternans of the Iberian Peninsula

In the last century, the presence of two species of hadrosauriforms in the Barremian of England has been accepted until the description in 2021 of *Brighstoneus simmondsi*: the large-sized and robust *Iguanodon bernissartensis* and the medium-sized and gracile *Mantellisaurus atherfieldensis* (Norman, 2013; Lockwood et al., 2021). Meanwhile in Spain several species have been identified, including the two historical taxa from England (Fig. 8). Verdú et al. (2019) grouped the basal hadrosauriforms of the Iberian Peninsula into two morphotypes based on morphometric analysis. The large-sized hadrosauriforms could include *I. bernissartensis*, *I. galvensis*, *M. soriaensis* and the *nomen dubium D. turolensis*, whereas a medium-sized morphogroup could be formed by *M. atherfieldensis*, *M. beltrani* and *P. sosbaynati*. The described taxon would be related to the medium-sized ornithopod morphotype proposed by Verdú et al. (2019).

The palaeogeographical distribution of iberian taxa is bounded to the different basins or sub-basins deposited during the Lower Cretaceous (fig. 8), while other European taxa like *I. bernissartensis* and *M. atherfieldensis* have a more widespread distribution. The assignment of new genera or species based on incomplete specimens could lead to an overestimation of the Hadrosauriformes

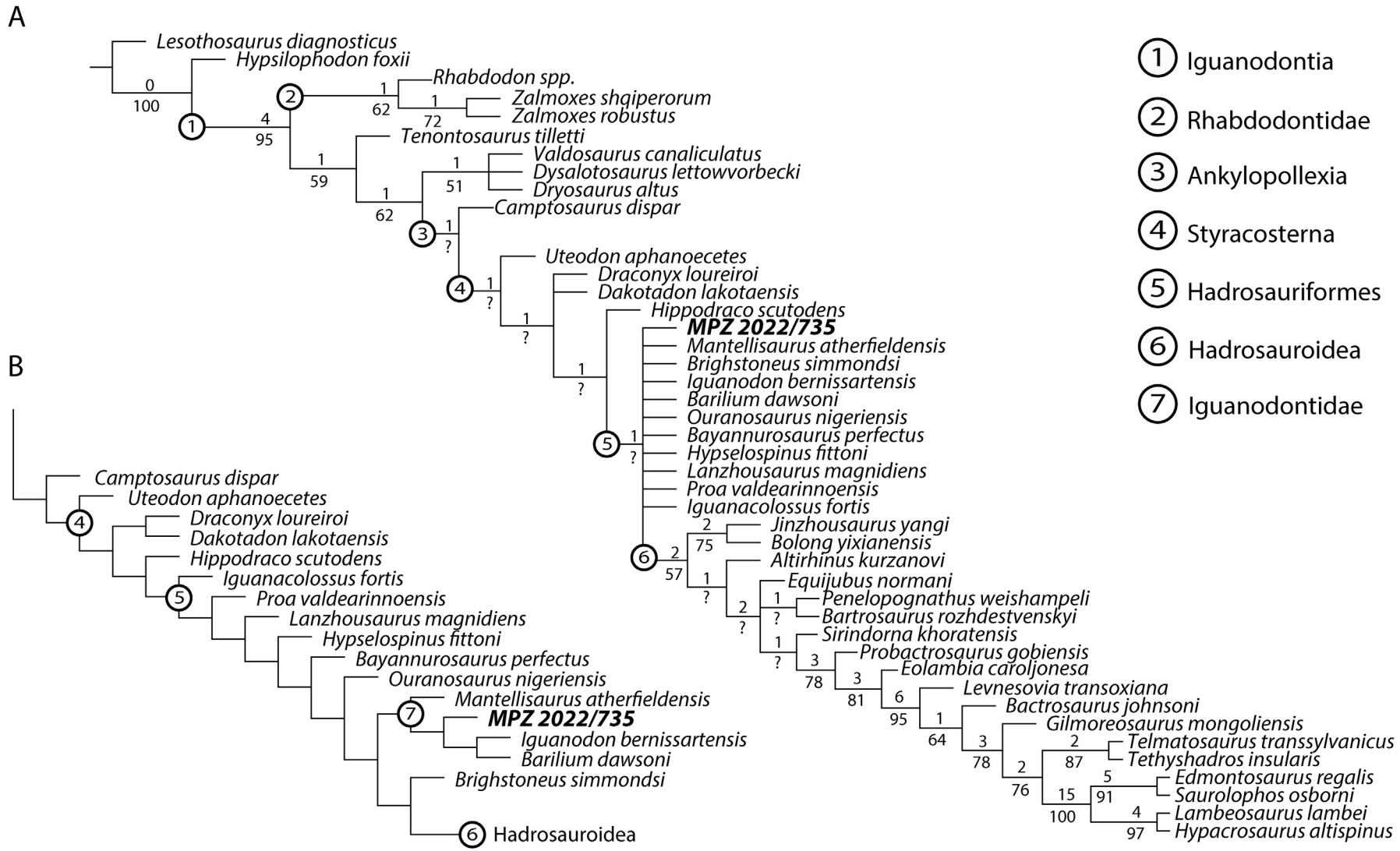

Fig. 7. Strict consensus tree and implied weight search cladogram of the Rotatori et al. (2022) matrix after the addition of MPZ 2022/735. A. Strict consensus tree of the matrix showing the position of MPZ 2022/735 in the basal Hadrosauriformes polytomy with bootstrap value (below, under 50 an "?" is shown) and Bremer support (above). B. Cladogram based on the implied weight search using a concavity constant of 15 with MPZ 2022/735 included in the Iguanodontidae clade as a sister taxon to *Mantellisaurus atherfieldensis* and *Iguanodon bernissartensis* and *Barilium dawsoni*.

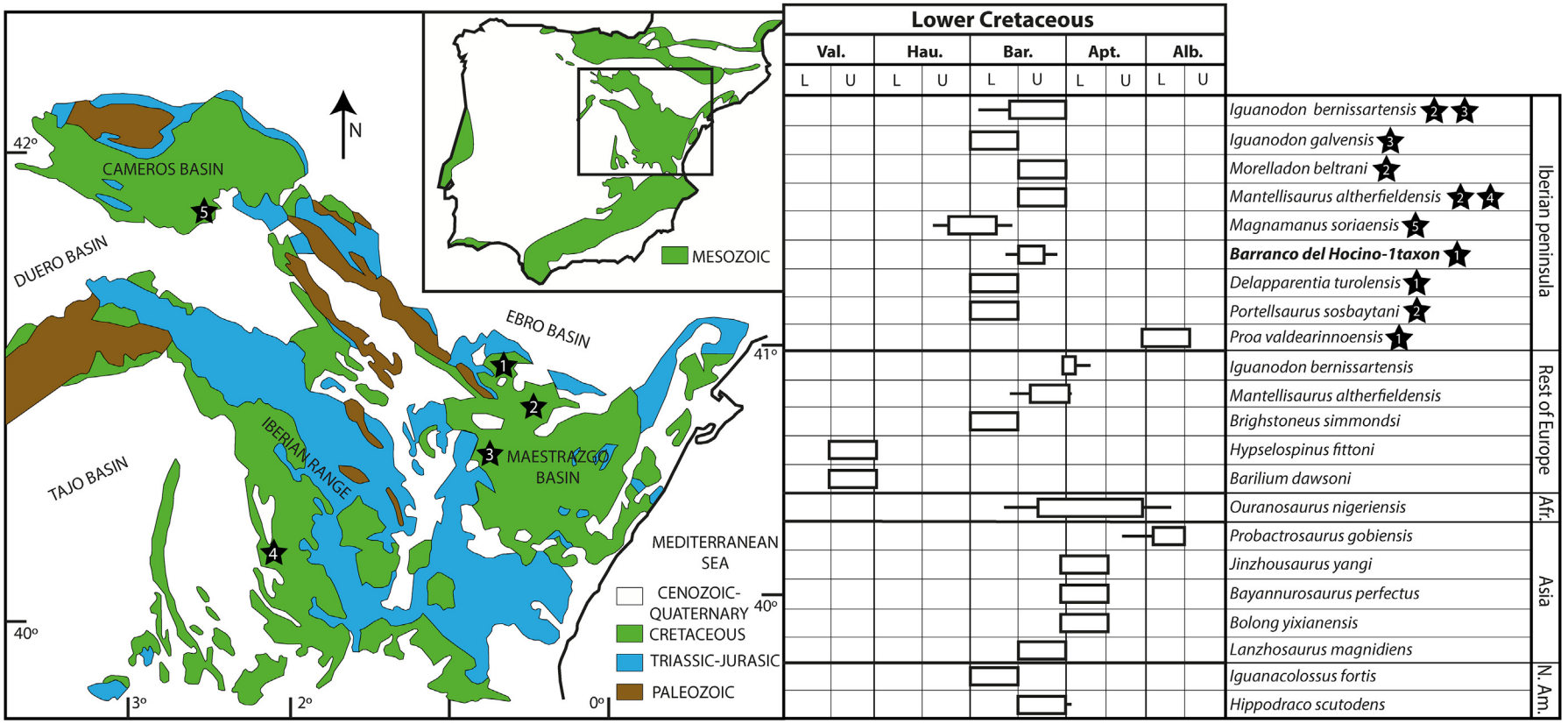

Fig. 8. Geographical and temporal distribution of the basal hadrosauriform dinosaurs of the Iberian Peninsula and temporal distribution of closely related taxa in the rest of Europe, Africa, Asia and North America. Left: Map of the Iberian Peninsula. Stars are for the different geological formations with hadrosauriform fossils that have been referred to a taxon. Star formations: 1, Blesa Formation (*Delapparentia turolensis* and Barranco del hocino-1 site) and Escucha Formation (*Proa valdearinnoensis*); 2, Arcillas de Morella Formation; 3, Camarillas Formation; 4, Las Hoyas Lagerstätte; and 5, Golmayo Formation. Right: Table with the ornithopod taxa distributed in time and grouped by continents with special attention paid to the iberian taxa.

diversity in the area. However, the temporal distance of the different formations in different basins of the same age could be millions of years, long enough for a species replacement (Prothero, 2014; Blanco et al., 2021). In the phylogenetic analysis published by Gasulla et al. (2015) and Verdú et al. (2017), the genus *Iguanodon* is a sister taxon to *Barilium dawsoni*, whereas *Morelladon beltrani* is a sister taxon to *Mantellisaurus atherfieldensis*. As described above, the general morphology of the ilium MPZ 2022/735 is close to the genus *Iguanodon*, whereas the smaller size could be more related with the taxa *M. beltrani* and *M. atherfieldensis*. Our phylogenetic analysis shows a similar result, recovering the ornithopod of Barranco del Hocino-1 site as the sister taxon to *M. atherfieldensis* and a clade formed by *B. dawsoni* and *Iguanodon bernissartensis*. *Portellsaurus sosbaynati* has been described from a partial dentary, and *Magnamanus soriaensis* only has ribs and vertebrae as overlapping material for comparison. Future revisions of Hadrosauriformes from the Barremian/Aptian of the Iberian Peninsula, including all the taxa together in the same matrix, could shed light on the relationships among them and on the diversity of the medium-large ornithopods of the Early Cretaceous.

7. Conclusions

The Blesa Formation is well known for the great wealth of fossils, especially vertebrate remains. In spite of the numerous fossiliferous sites found in the Lower and Middle Blesa sequences, most of the remains recovered are isolated and fragmentary. The hadrosauriforme of Barranco del Hocino-1 site represents the most complete ornithopod known in this geological formation and the first recovered in the Upper Blesa Sequence.

A unique combination of characters from caudal vertebrae, ribs and ilium allows the described fossils to be differentiated from the basal styracosternan ornithopods of the Lower Cretaceous.

The phylogenetic analysis on the basis of some characters of the ilium recovers the Barranco del Hocino-1 ornithopod as a member of Iguanodontidae with *Barilium dawsoni*, *Iguanodon bernissartensis* and *Mantellisaurus atherfieldensis*. The results of the cladistic analysis should be treated with caution given the scarce number of characters that have been codified for this ornithopod but they reinforce the results obtained in the study of the morphological characters. We consider the ornithopod of Barranco del Hocino-1 site as a potentially new taxon considering that the bones described would correspond to the same individual but the taphonomic conditions prevents us from confirming the latter with complete certainty.

The presence of a new possible styracosternan ornithopod in the Barremian of the Iberian Peninsula adds to the ornithopod richness during the Early Cretaceous of the southwest of Europe. The relative high ornithopod diversity and abundance of this paleogeographic region would be indicative of it could have played an important role for the biogeographical and evolutionary history of this dinosaur group.

Funding

This study was subsidized by the Spanish Ministerio de Economía y Competitividad (project CGL2017-85038-P), the Spanish Ministerio de Ciencia e innovación (project PID2021-122612OB-I00), and by the Aragón Regional Government and European Regional Development Fund (research group E18_20R Aragosaurus: recursos geológicos y paleoambientes). Eduardo Medrano Aguado has a predoctoral contract financed by the Aragón Government.

Data availability

Data will be made available on request.

Acknowledgements

We want to acknowledge Carmen Núñez, Pablo Navarro, Ester Díaz, Manuel Pérez, Erik Isasmendi and specially Juan and Cristóbal Rubio and their families for their collaboration in the fieldwork campaigns. Australair S.L. cofounded some of the field campaigns. I. Pérez helps with the photography of the fossils. R. Glasgow reviewed the text in English. Finally, we are grateful to Xabier Pereda-Suberbiola, two other anonymous reviewers, and the editor Eduardo Koutsoukos, for their exhaustive comments, which have greatly enhanced the quality of this paper.

References

Alonso, A., Canudo, J.I., 2015. On the spinosaurid theropod teeth from the early Barremian (Early Cretaceous) Blesa Formation (Spain). Historical Biology 28 (6), 823–834. https://doi.org/10.1080/08912963.2015.1036751.

Alonso, A., Gasca, J.M., Navarro-Lorbés, P., Núñez-Lahuerta, C., Galán, J., Parrilla-Bel, J., Rubio, C., Canudo, J.I., 2016. La asociación faunística de Barranco del Hocino 1, un nuevo yacimiento de vertebrados del Barremiense (Cretácico Inferior) de Teruel. Cuadernos Del Museo Geominero 20, 303–307.

Alonso, A., Gasca, J.M., Navarro-Lorbés, P., Rubio, C., Canudo, J.I., 2018. A new contribution to our knowledge of the large-bodied theropods from the Barremian of the Iberian Peninsula: the "Barranco del Hocino" site (Spain). Journal of Iberian Geology 44 (1), 7–23. https://doi.org/10.1007/s41513-018-0051-9.

Aurell, M., Soria, A.R., Bádenas, B., Liesa, C.L., Canudo, J.I., Gasca, J.M., Moreno-Azanza, M., Medrano-Aguado, E., Meléndez, A., 2018. Barremian synrift sedimentation in the Oliete sub-basin (Iberian Basin, Spain): palaeogeographical evolution and distribution of vertebrate remains. Journal of Iberian Geology 44 (2), 285–308. https://doi.org/10.1007/s41513-018-0057-3.

Bertozzo, F., Dalla Vecchia, F.M., Fabbri, M., 2017. The Venice specimen of *Ouranosaurus nigeriensis* (Dinosauria, Ornithopoda). PeerJ 2017 (6), 1–70. https://doi.org/10.7717/peerj.3403.

Blanco, F., Calatayud, J., Martín-Perea, D.M., Domingo, M.S., Menéndez, I., Müller, J., Fernández, M.H., Cantalapiedra, J.L., 2021. Punctuated ecological equilibrium in mammal communities over evolutionary time scales. Science 372 (6539), 300–303.

Boyd, C.A., 2015. The systematic relationships and biogeographic history of ornithischian dinosaurs. PeerJ 2015 (12). https://doi.org/10.7717/peerj.1523.

Canudo, J.I., 2018. The collection of type fossils of the Natural Science Museum of the University of Zaragoza (Spain). Geoheritage 10 (3), 385–392.

Canudo, J.I., Gasca, J.M., Aurell, M., Badiola, A., Blain, H.-A., Cruzado-Caballero, P., Gómez-Fernández, D., Moreno-Azanza, M., Parrilla-Bel, J., Rabal-Garcés, R., Ruiz-Omeñaca, J.I., 2010. La Cantalera: an exceptional window onto the vertebrate biodiversity of the Hauterivian-Barremian transition in the Iberian Peninsula. Journal of Iberian Geology 36 (2), 205–224. https://doi.org/10.5209/rev.

Carpenter, K., Ishida, Y., 2010. Early and Middle Cretaceous iguanodonts in time and space. Journal of Iberian Geology 36 (2), 145–164. https://doi.org/10.5209/rev_JIGE.2010.v36.n2.3.

Forster, C.A., 1990. The postcranial skeleton of the ornithopod dinosaur *Tenontosaurus tilletti*. Journal of Vertebrate Paleontology 10, 273–294.

Fuentes Vidarte, C., Meijide Calvo, M., Meijide Fuentes, F., Meijide Fuentes, M., 2016. Un nuevo dinosaurio estiracosterno (Ornithopoda: Ankylopollexia) del Cretácico Inferior de España. Spanish Journal of Palaeontology 31 (2), 407. https://doi.org/10.7203/sjp.31.2.17163.

García-Cobeña, J., Verdú, F.J., Cobos, A., 2022. Abundance of large ornithopod dinosaurs in the El Castellar Formation (Hauterivian-Barremian, Lower Cretaceous) of the Peñagolosa sub-basin (Teruel, Spain). Journal of Iberian Geology, 0123456789. https://doi.org/10.1007/s41513-021-00185-w.

García-Penas, A., Aurell, M., Zamora, S., 2022. Progressive opening of a shallow-marine bay (Oliete Subbasin, Spain) and the record of possible eustatic fall events near the Barremian-Aptian boundary. Palaeogeography, Palaeoclimatology, Palaeoecology 594, 110938.

Gasca, J.M., Moreno-Azanza, M., Ruiz-Omeñaca, J.I., Canudo, J.I., 2015. New material and phylogenetic position of the basal iguanodont dinosaur *Delapparentia turolensis* from the Barremian (Early Cretaceous) of Spain. Journal of Iberian Geology 41 (1), 57–70. https://doi.org/10.5209/rev_JIGE.2015.v41.n1.48655.

Gasca, José Manuel, Canudo, J.I., Moreno-Azanza, M., 2014. On the diversity of Iberian iguanodont dinosaurs: new fossils from the lower Barremian, Teruel province, Spain. Cretaceous Research 50, 264–272. https://doi.org/10.1016/j.cretres.2014.05.009.

Gasulla, J.M., 2015. Los dinosaurios de la Cantera del Mas de la Parreta, Morella (Formación Morella, Barremiense superior, Cretácico Inferior): sistemática, análisis filogenético e implicaciones paleobiológicas. Ph.D. dissertation. Universidad Autónoma de Madrid, Madrid, Spain, p. 279.

Gasulla, J.M., Escaso, F., Narváez, I., Luis Sanz, J., Ortega, F., 2022. New *Iguanodon bernissartensis* axial bones (Dinosauria, Ornithopoda) from the Early Cretaceous of Morella, Spain. Diversity 14 (2), 63. https://doi.org/10.3390/d14020063.

Gasulla, J.M., Escaso, F., Narváez, I., Ortega, F., Sanz, J.L., 2015. A new sail-backed styracosternan (Dinosauria: Ornithopoda) from the Early Cretaceous of Morella, Spain. PLoS One 10 (12), 1–27. https://doi.org/10.1371/journal.pone.0144167.

Godefroit, P., Dong, Z.M., De Potter, H., Lenglet, G., Smith, T., Dermience, E., 1998. Sino-Belgian Cooperation Program Cretaceous dinosaurs and mammals from inner Mongolia. 1. New *Bactrosaurus* (Dinosauria: Hadrosauroidea) material from Iren Dabasu (inner Mongolia, PR China). Bulletin-Institut royal des sciences naturelles de Belgique. Sciences de la terre 68, 3–70.

Godefroit, P., Codrea, V., Weishampel, D.B., 2009. Osteology of *Zalmoxes shqiperorum* (Dinosauria, Ornithopoda), based on new specimens from the Upper Cretaceous of Nălaţ-Vad (Romania). Geodiversitas 31 (3), 525–553. https://doi.org/10.5252/g2009n3a3.

Godefroit, P., Loeuff, J.L., Carlier, P., Pirson, S., Yans, J., Suteethorn, S., Spagna, P., 2012. Early Cretaceous dinosaur remains from Baudour (Belgium). In: Godefroit, P. (Ed.), Bernissart Dinosaurs and Early Cretaceous Terrestrial Ecosystems. Indiana University Press, Bloomington and Indianapolis, pp. 147–157.

Goloboff, P.A., Catalano, S.A., 2016. TNT v.1.5, including a full implementation of phylogenetic morphometrics. Cladistics 32, 221–238.

Goloboff, P.A., Carpenter, J.M., Arias, J.S., Esquivel, D.R.M., 2008. Weighting against homoplasy improves phylogenetic analysis of morphological data sets. Cladistics 24 (5), 758–773.

Holgado, B., Pêgas, R.V., Canudo, J.I., Fortuny, J., Rodrigues, T., Company, J., Kellner, A.W., 2019. On a new crested pterodactyloid from the Early Cretaceous of the Iberian Peninsula and the radiation of the clade Anhangueria. Scientific Reports 9 (1), 1–10.

Horner, J.R., Weishampel, D.B., Forster, C.A., 2004. Hadrosauridae. In: Weishampel, B., Dodson, P., Osmólska, H. (Eds.), The Dinosauria. University of California Press, Berkeley, CA, pp. 438–463.

Hübner, T.R., 2018. The postcranial ontogeny of *Dysalotosaurus lettowvorbecki* (Ornithischia: Iguanodontia) and implications for the evolution of ornithopod dinosaurs. Palaeontographica Abteilung A: Paläozoologie-Stratigraphic 310 (3–6), 43–120.

Lockwood, J.A.F., Martill, D.M., Maidment, S.C.R., 2021. A new hadrosauriform dinosaur from the Wessex Formation, Wealden Group (Early Cretaceous), of the Isle of Wight, southern England. Journal of Systematic Palaeontology 19 (12), 847–888. https://doi.org/10.1080/14772019.2021.1978005.

Maddison, W.P., Maddison, D.R., 2018. Mesquite: a modular system for evolutionary analysis. Version 3.6.

Marsh, O.C., 1881. Principal characters of American Jurassic dinosaurs. Part V. American Journal of Science (Series 3) 21, 417–423.

McDonald, A.T., 2010. A new basal iguanodont (Dinosauria: Ornithischia) from the Wealden. Zootaxa 2569, 1–43. https://doi.org/10.5281/zenodo.197354.

McDonald, A.T., 2011. The taxonomy of species assigned to Camptosaurus (Dinosauria: Ornithopoda). Zootaxa 68 (2783), 52–68. https://doi.org/10.11646/zootaxa.2783.1.4.

McDonald, A.T., 2012. Phylogeny of basal iguanodonts (Dinosauria: Ornithischia): an update. PLoS One 7 (5). https://doi.org/10.1371/journal.pone.0036745.

McDonald, A.T., Espilez, E., Mampel, L., Kirkland, J.I., Alcala, L., 2012. An unusual new basal iguanodont (Dinosauria: Ornithopoda) from the Lower Cretaceous of Teruel, Spain. Zootaxa 3595 (2012), 61–76.

Medrano-Aguado, E., Parrilla-Bel, J., Gasca, J.M., Alonso, A., Canudo, J.I., 2021. Ornithopod palaeobiodiversity in the Barranco del Hocino-1 site, from the upper Barremian in the Oliete subbasin (Teruel, Spain). Ciências da Terra Procedia 1 (2021), 58–61. https://doi.org/10.21695/cterraproc.v1i0.408.

Norman, D.B., 1980. On the ornithischian dinosaur *Iguanodon bernissartensis* from the Lower Cretaceous of Bernissart (Belgium). Mémoires Institut Royal Des Sciences Naturelles de Belgique 178, 1–103.

Norman, D.B., 1986. On the anatomy of *Iguanodon atherfieldensis* (Ornithischia: Ornithopoda). Bulletin de l'Institut Royal des Sciences Naturelles de Belgique 56, 281–372.

Norman, D.B., 2004. Basal Iguanodontia. In: Weishampel, D.B., Dodson, P., Osmolska, H. (Eds.), The Dinosauria. University of California, Berkeley, pp. 413–437.

Norman, D.B., 2011. On the osteology of the lower Wealden (Valanginian) ornithopod *Barilium dawsoni* (Iguanodontia: Styracosterna). Special Papers in Palaeontology 86, 165–194. https://doi.org/10.1111/J.1475-4983.2011.01082.x.

Norman, D.B., 2013. On the taxonomy and diversity of Wealden iguanodontian dinosaurs (Ornithischia: Ornithopoda). Revue de Paleobiologie 32 (2), 385–404.

Norman, D.B., 2015. On the history, osteology, and systematic position of the Wealden (Hastings group) dinosaur Hypselospinus fittoni (Iguanodontia: Styracosterna). Zoological Journal of the Linnean Society 173 (1), 92–189. https://doi.org/10.1111/zoj.121.

Owen, R., 1842. Report on British fossil reptiles. Part II. In: Report of the Eleventh Meeting of the British Association for the Advancement of Science, Plymouth, England, July 1841. John Murray, London, pp. 60–204.

Parrilla-Bel, J., Canudo, J.I., 2015. On the presence of plesiosaurs in the Blesa Formation (Barremian) in Teruel (Spain). Neues Jahrbuch für Geologie und Paläontologie - Abhandlungen 278 (2), 213–227.

Parrilla-Bel, J., Medrano-Aguado, E., Puértolas-Pascual, E., Canudo, J.I., 2022. Crocodylomorph diversity in Barranco del Hocino-1 site (Barremian, Lower Cretaceous) in Estercuel (Teruel, Spain). In: 9th Symposium about Dinosaur Paleontology and their Environment. Salas de los Infantes, España. 7-10 September, 2022.

Paul, G.S., 2008. A revised taxonomy of the iguanodont dinosaur genera and species. Cretaceous Research 29 (2), 192–216.

Pereda-Suberbiola, X., Ruiz-Omeñaca, J.I., Torcida Fernández-Baldor, F., Maisch, M.W., Huerta, P., Contreras, R., Izquierdo, L.Á., Huerta, D.M., Montero, V.U., Welle, J., 2011. A tall-spined ornithopod dinosaur from the Early Cretaceous of Salas de los Infantes (Burgos, Spain). Comptes Rendus Palevol 10 (7), 551–558. https://doi.org/10.1016/j.crpv.2011.04.003.

Prothero, D.R., 2014. Species longevity in North American fossil mammals. Integrative Zoology 9 (4), 383–393.

Riveline, J., Berger, J.P., Feist, M., Martín-Closas, C., Schudack, M., Soulié-Märsche, I., 1996. European Mesozoic-Cenozoic charophyte biozonation. Bulletin de la Société géologique de France 167 (3), 453–468.

Rotatori, F.M., Moreno-Azanza, M., Mateus, O., 2022. Reappraisal and new material of the holotype of *Draconyx loureiroi* (Ornithischia: Iguanodontia) provide insights on the tempo and modo of evolution of thumb-spiked dinosaurs. Zoological Journal of the Linnean Society 195 (1), 125–156.

Ruiz-Omeñaca, J.I., 2011. *Delapparentia turolensis* nov. gen et sp., un nuevo dinosaurio iguanodontoideo (Ornithischia: Ornithopoda) en el Cretácico Inferior de Galve. Estudios Geologicos 67 (1), 83–110. https://doi.org/10.3989/egeol.40276.124.

Salas, R., Guimerà, J., Mas, R., Martín-Closas, C., Meléndez, A., Alonso, A., 2001. Evolution of the Mesozoic Central Iberian Rift System and its Cainozoic inversion (Iberian chain). Mémoires du Muséum National d'Histoire Naturelle 186, 145–186.

Sanguino, F., Buscalioni, A.D., 2018. The *Iguanodon* locality of Pata la Mona (upper Barremian, Buenache de la Sierra, Cuenca) revisited. In: Proceedings of the XVI Encuentro de Jóvenes Investigadores en Paleontología, Zarautz, Spain, 11–14 April 2018, pp. 103–106.

Santos-Cubedo, A., De Santisteban, C., Poza, B., Meseguer, S., 2021. A new styracosternan hadrosauroid (Dinosauria: Ornithischia) from the Early Cretaceous of Portell, Spain. PLoS One 16 (7 July 2021), 1–30. https://doi.org/10.1371/journal.pone.0253599.

Seeley, H.G., 1887. On the classification of the fossil animals commonly called Dinosauria. Proceedings of the Royal Society of London 43, 165–171.

Sereno, P.C., 1986. Phylogeny of the bird-hipped dinosaurs (order Ornithischia). National Geographic Research 2, 234–256.

Serrano, M.L., Vullo, R., Marugán-Lobón, J., Ortega, F., Buscalioni, Á.D., 2013. An articulated hindlimb of a basal iguanodont (Dinosauria, Ornithopoda) from the Early Cretaceous Las Hoyas Lagerstätte (Spain). Geological Magazine 150 (3), 572–576. https://doi.org/10.1017/S0016756813000095.

Soria, A., Martín-Closas, C., Meléndez, a, Meléndez, M., Aurell, M., 1995. Estratigrafía del Cretácico Inferior continental de la Cordillera Ibérica Central. Estudios Geológicos 152 (51), 141–152.

Verdú, F.J., 2017. Sistemática, filogenia y paleobiología de *Iguanodon galvensis* (Ornithopoda, Dinosauria) del Barremiense inferior (Cretácico Inferior) de Teruel (España). Ph.D. dissertation. University of Valencia, Valencia, Spain, p. 445.

Verdú, F.J., Cobos, A., Royo-Torres, R., Alcalá, L., 2019. Diversity of large ornithopod dinosaurs in the upper Hauterivian-lower Barremian (Lower Cretaceous) of Teruel (Spain): a morphometric approach. Spanish Journal of Paleontology 34 (2), 269–288. https://doi.org/10.7203/sjp.34.2.16116.

Verdú, F.J., Godefroit, P., Royo-Torres, R., Cobos, A., Alcala, L., 2017. Individual variation in the postcranial skeleton of the Early Cretaceous *Iguanodon bernissartensis* (Dinosauria: Ornithopoda). Cretaceous Research 74, 65–86.

Verdú, F.J., Royo-Torres, R., Cobos, A., Alcalá, L., 2018. New systematic and phylogenetic data about the early Barremian *Iguanodon galvensis* (Ornithopoda: Iguanodontoidea) from Spain. Historical Biology 30 (4), 437–474. https://doi.org/10.1080/08912963.2017.1287179.

Weishampel, D.B., Dodson, P., Osmólska, H. (Eds.), 2004. The Dinosauria. Univ of California Press.

Weishampel, D.B., Jianu, C.M., Csiki, Z., Norman, D.B., 2003. Osteology and phylogeny of *Zalmoxes* (n. g.), an unusual Euornithopod dinosaur from the latest Cretaceous of Romania. Journal of Systematic Palaeontology 1 (2), 65–123. https://doi.org/10.1017/S1477201903001032.

Xu, X., Tan, Q., Gao, Y., Bao, Z., Yin, Z., Guo, B., Wang, J., Tan, L., Zhang, Y., Xing, H., 2018. A large-sized basal ankylopollexian from East Asia, shedding light on early biogeographic history of Iguanodontia. Science Bulletin 63 (9), 556–563. https://doi.org/10.1016/j.scib.2018.03.016.

Appendix A. Supplementary data

Supplementary data to this article can be found online at https://doi.org/10.1016/j.cretres.2022.105458.